JACS
JOURNAL OF THE AMERICAN CHEMICAL SOCIETY

Article

pubs.acs.org/JACS

Real-Time Monitoring of Cell Apoptosis and Drug Screening Using Fluorescent Light-Up Probe with Aggregation-Induced Emission Characteristics

Haibin Shi,[†,‡] Ryan T. K. Kwok,[#,‡] Jianzhao Liu,[#] Bengang Xing,[∥] Ben Zhong Tang,*[,#,§,⊥] and Bin Liu*[,†,§]

[†]Department of Chemical and Biomolecular Engineering, 4 Engineering Drive 4, National University of Singapore, Singapore 117576

[#]Department of Chemistry, Institute for Advanced Study, Division of Biomedical Engineering, State Key Laboratory of Molecular Neuroscience and Institute of Molecular Functional Materials, The Hong Kong University of Science and Technology, Clear Water Bay, Kowloon, Hong Kong, China

[⊥]Guangdong Innovative Research Team, State Key Laboratory of Luminescent Materials and Devices, South China University of Technology, Guangzhou 510640, China

[§]Institute of Materials Research Engineering, 3 Research Link, Singapore 117602

[∥]Division of Chemistry and Biological Chemistry, School of Physical and Mathematical Sciences, Nanyang Technological University, Singapore 637371

Supporting Information

ABSTRACT: Real-time monitoring of cell apoptosis could provide valuable insights into early detection of therapy efficiency and evaluation of disease progression. In this work, we designed and synthesized a new live-cell-permeable, fluorescent light-up probe for real-time cell apoptosis imaging. The probe is comprised of a hydrophilic caspase-specific Asp-Glu-Val-Asp (DEVD) peptide and a hydrophobic tetraphenylethene (TPE) unit, a typical fluorogen with aggregation-induced emission characteristics. In aqueous solution, the probe is almost nonfluorescent but displays significant fluorescence enhancement in response to caspase-3/-7, which are activated in the apoptotic process and able to cleave the DEVD moieties. This fluorescence "turn-on" response is ascribed to aggregation of cleaved hydrophobic TPE residues, which restricts the intramolecular rotations of TPE phenyl rings and populates the radiative decay channels. The light-up nature of the probe allows real-time monitoring of caspase-3/-7 activities both in solutions and in living cells with a high signal-to-noise ratio. The probe provides a new opportunity to screen enzyme inhibitors and evaluate the apoptosis-associated drug efficacy.

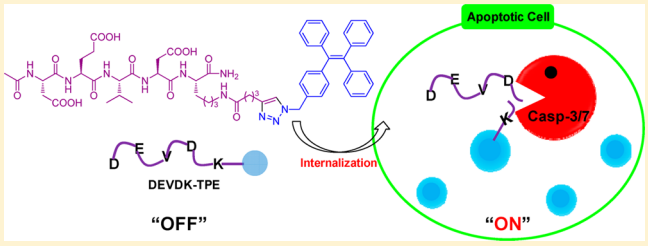

INTRODUCTION

Apoptosis, or programmed cell death, is an important and active regulatory pathway of cell growth and proliferation.[1,2] Deregulation of the cell apoptosis can ultimately lead to cancers, neurodegenerative diseases, autoimmune diseases, atherosclerosis, myocardial infarction, and many other diseases.[3,4] Real-time imaging the progress of apoptosis in living organisms therefore has great implications for early diagnosis of diseases, evaluation of disease progression and therapy efficiency, and screening of apoptosis-related drugs.[5]

Cells undergoing apoptosis generally show characteristic biochemical changes, which include translocation of phosphatidylserine (PS) from the cytoplasmic leaflet to the extracellular leaflet of the plasma membrane, DNA fragmentation, protease activation, and so on.[6] So far, a number of strategies have been attempted to monitor the apoptosis progress.[7−10] One common approach is to target the negatively charged PS with annexin V by taking advantage of the specific binding between them.[7,11] However, false positive results have been reported because PS exposure also occurs in other biological processes, like necrosis.[12] Laddering of DNA fragmentation is another widely used method for apoptosis monitoring. It requires multiple reaction steps, and the internucleosomal DNA cleavages are not always associated with apoptosis.[13,14] To overcome the limitations of these methods, assays for more specific key players in the apoptosis, such as caspases, have recently received considerable attention.

Caspases are a family of intracellular cysteine proteases that play critical roles in the initiation and execution of apoptosis.[4,15−17] Among them, caspase-3 has been identified as a key mediator of cell apoptosis, and it becomes an attractive and unambiguous target for apoptosis imaging. So far, two major groups of fluorescent probes have been developed to monitor caspase activities.[18−23] The first group refers to fluorogenic probes containing caspase-specific peptide sub-

Received: July 3, 2012
Published: October 8, 2012

   dx.doi.org/10.1021/ja3064588 | J. Am. Chem. Soc. 2012, 134, 17972−17981

strates and luciferin or luciferase[19] or latent fluorophores.[20] Fluorogenic peptide substrates containing C-terminally capped coumarin derivative (i.e., 7-amino-4-trifluoromethylcoumarin (AFC)) are arguably the most useful probes for substrate specificity profiling experiments, as the cleavage at the amide bond between the peptide and the coumarin moiety will release the fluorescent coumarin.[20] However, these fluorogenic probes have not been effective for cell apoptosis imaging due to high fluorescence background and poor cell permeability. The second group is dual-labeled probes, which rely on functionalization of the caspase-specific peptide substrates with donor/quencher pairs[18,21,22] or fluorescence resonance energy transfer (FRET) pairs on both ends.[23] Peptide cleavage by caspases can result in separation of dye/quencher pair or loss of FRET, which enables the caspase activities to be evaluated via the changes in fluorescence intensity and wavelength. Although the dual-labeled probes have overcome some disadvantages of fluorogenic probes, they require more complicated synthetic steps, and the background signal is highly dependent on the quenching efficiency or FRET efficiency. Given the above considerations, it is highly desirable to develop much simpler, noninvasive, and specific probes with high signal-to-noise ratio for real-time monitoring of cell apoptosis and direct evaluation of new apoptosis-related drugs in living cells.

Aggregation-induced emission (AIE) is a unique photophysical phenomenon that was first reported in 2001.[24] Propeller-shaped fluorogens, such as tetraphenylethene (TPE), are nonemissive when molecularly dissolved in solution but induced to emit efficiently by aggregate formation.[25] We have rationalized the AIE mechanism as restriction of intramolecular rotations (RIR) in the aggregate state.[26] To date, a variety of fluorogens with AIE characteristics have been developed for applications in chemical sensors,[25b,27,28] biological imaging,[29] and optoelectronic devices.[26a,30] Of particular importance is that the AIE phenomenon has been demonstrated to be useful in monitoring activities of various enzymes, such as trypsin,[31] acetylcholinesterase (AChE),[32] and alkaline phosphatase.[33] These assays rely on weakly fluorescent AIE fluorogens in solutions to interact with oppositely charged chemical or protein substrates to yield fluorescent complexes, which then release the AIE fluorogens back to the solutions upon enzyme digestion and lead to fluorescence "turn-off". Although many efforts have also been made to develop AIE-based fluorescence "turn-on" assays for enzyme activity studies,[34] multiple reagents or chemical reactions have to be involved, which make them also not suitable for cellular based studies.

In this contribution, we designed and synthesized a probe via conjugation between a hydrophilic DEVD peptide sequence and a hydrophobic AIE fluorogen. The probe is highly water-soluble and nonfluorescent in aqueous environment. The specific cleavage of DEVD by caspase-3/-7 induces aggregation of the hydrophobic AIE residues and thus enhances the fluorescence signal output. This probe is capable of detecting caspase-3/-7 activities both in solution and in living cells. By monitoring the activity of caspase-3 in living cells, we further demonstrated that our probe could be used for real-time apoptosis imaging and *in situ* apoptosis-related drug screening with high fluorescence contrast.

RESULTS AND DISCUSSION

Design Principle of AIE-based Probe. TPE is a classic AIE fluorogen that emits strongly in aggregate state but shows very weak fluorescence in dilute solutions.[25] This is due to the propeller-shaped structure of TPE, and the dynamic rotations of the phenyl rings nonradiatively deactivated their excited states in solution. In the aggregate state, the RIR due to the physical constraint in the aggregates opens the radiative decay channel.[26] Our design rationale is illustrated in Scheme 1. The

Scheme 1. Illustration of Ac-DEVDK-TPE for Caspase Activities Study

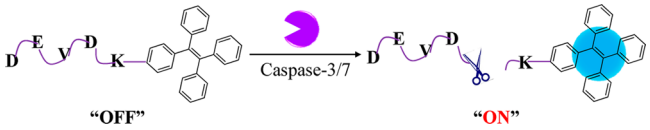

acetyl protective N-terminal Asp-Glu-Val-Asp-Lys-TPE probe (Ac-DEVDK-TPE) is made of three components: (1) a DEVD sequence that can be specifically cleaved by caspase-3/-7 and used to endow the probe with water solubility; (2) an azide-functionalized TPE fluorogen with modulated fluorescence *on/off* upon external stimuli; and (3) an alkyne-functionalized lysine derivative as a linker to connect DEVD and TPE moieties. Ac-DEVDK-TPE is highly water-soluble and displays very weak fluorescence in aqueous media due to the consumption of excitonic energy by the active intramolecular rotations.[24,25] It is hypothesized that once the probe is internalized into apoptotic cells, the DEVD moiety will be specifically cleaved between Asp(D) and Lys(K) by caspase-3/-7, leading to the release of lysine-conjugated TPE (K-TPE). As K-TPE is hydrophobic, molecular aggregation will lead to fluorescence turn-on according to the AIE mechanism.[24,25] Therefore, the probe provides a good opportunity for real-time imaging of apoptosis process.

Synthesis and Characterization of Probe Ac-DEVDK-TPE. The synthesis of Ac-DEVDK-TPE probe involves both solution- and solid-phase chemistry as described in Schemes 2 and 3. Azide-functionalized tetraphenylethene (**3**, TPE-N_3) was synthesized in four steps with a 45% total yield. Detailed synthesis and characterization of TPE-N_3 and the intermediates are shown in the Experimental Section and Supporting Information (Figures S1−S6). The alkyne-bearing Ac-DEVDK (Ac-DEVDK-A) peptide was prepared by standard solid-phase fluorenylmethoxy)carbonyl (Fmoc) peptide chemistry.[18d] In brief, deprotection of Fmoc group with 20% piperidine in dimethylformamide (DMF) yielded amine-functionalized rink amide resin, which was coupled to the first amino acid, alkyne-functionalized lysine, to afford the lysine-bearing resin. Following the same procedure, four different amino acids (Asp, Val, Glu, and Asp) were subsequently incorporated onto the resin by standard coupling reactions. Deprotection of the amine groups, followed by capping with acetic anhydride and cleaving from resin, gave the product Ac-DEVDK-A. It was further purified by HPLC and characterized with LC-MS. Subsequent coupling between TPE-N_3 and Ac-DEVDK-A via Cu(I)-catalyzed "click" reaction using $CuSO_4$/sodium ascorbate as the catalyst and dimethyl sulfoxide (DMSO)/water as the solvent afforded the probe Ac-DEVDK-TPE in 70% yield after HPLC purification. The purity and identity of the probe have been fully characterized by analytical HPLC, NMR, and HR-MS (Figures S7 and S8).

The UV−vis absorption spectra of TPE-N_3 and Ac-DEVDK-TPE in DMSO/water (v/v = 1/199) are shown in Figure S9A. Both have a similar absorption profiles with an obvious

dx.doi.org/10.1021/ja3064588 | J. Am. Chem. Soc. 2012, 134, 17972−17981

Scheme 2. Synthetic Route to TPE-N_3

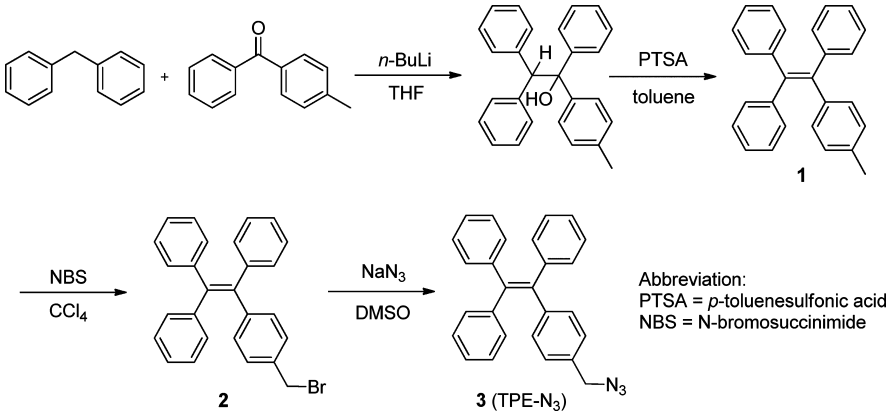

Scheme 3. Solid-Phase Synthesis of Ac-DEVDK-TPE[a]

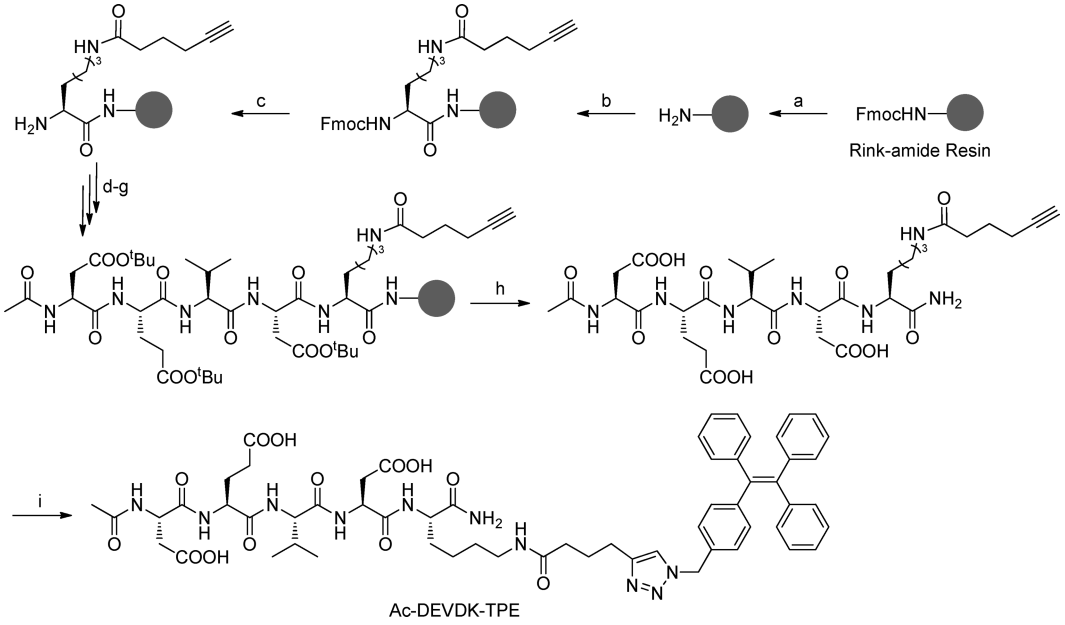

[a]Reagents and conditions: (a) 20% piperidine in DMF; (b) Fmoc-Lys(alkyne)-COOH, HBTU, HOBt, DIEA, DMF; (c) 20% piperidine in DMF; (d) i. Fmoc-Asp(O^{t}Bu)-OH, HBTU, HOBt, DIEA, DMF; ii. 20% piperidine in DMF; (e) i. Fmoc-Val-OH, HBTU, HOBt, DIEA, DMF; ii. 20% piperidine in DMF; (f) i. Fmoc-Glu(O^{t}Bu)-OH, HBTU, HOBt, DIEA, DMF; ii. 20% piperidine in DMF; (g) i. Fmoc-Asp(O^{t}Bu)-OH, HBTU, HOBt, DIEA, DMF; ii. 20% piperidine in DMF; iii. acetic anhydride, DIEA; (h) TFA/TIS/H_2O (v/v/v = 95:2.5:2.5), 3 h; (i) TPE-N_3 (1.0 equiv), $CuSO_4$ (0.2 equiv), sodium ascorbate (0.4 equiv) in DMSO/H_2O (1:1), 24 h. Abbreviations: HBTU, *O*-benzotriazole-*N*,*N*,*N*′,*N*′-tetramethyluronium hexafluorophosphate; HOBt, hydroxybenzotriazole; DIEA, *N*,*N*-diisopropylethylamine; TIS, triisopropylsilane.

absorbance in the 300−350 nm range. It is known that AIE fluorogen is virtually nonfluorescent in good solvents but emits intensely when aggregated in poor solvents. As can be seen from the photoluminescence (PL) spectra shown in Figure 1A, TPE-N_3, a hydrophobic AIE fluorogen, shows intense fluorescence as nanoaggregates in a mixture of DMSO/water (v/v = 1/199) with a quantum yield (Φ) of 0.2, while the Ac-DEVDK-TPE probe is almost nonfluorescent in the same medium (Φ = 0.001), due to its good solubility in water. The aggregate formation of the former and the molecular dissolution of the latter were confirmed by laser light scattering (LLS) measurements. In the aqueous mixture, the hydrophobic TPE-N_3 molecules cluster into aggregates with an average diameter of 126 nm (Figure S9B). No LLS signals, however, could be detected from the solution of Ac-DEVDK-TPE.

As biosensing is often conducted in buffers, it is important to study the effect of ionic strength on the emission behavior of the probe. The experiments were performed with addition of sodium chloride into an aqueous solution of Ac-DEVDK-TPE (10 μM). Almost no change in the PL spectrum of the probe is observed when the concentration of NaCl is increased from 0 to 960 mM (Figure S10). Clearly, ionic strength does not affect the fluorescence property of Ac-DEVDK-TPE. Its PL profile also does not change in the presence of the Dulbecco's Modified Eagle Medium (DMEM), which contains amino acids, salts, glucose, and vitamins. The probe maintains an "off" state in the complex environment and thus has great potential to serve as a specific light-up probe with minimum background interference.

Ac-DEVDK-TPE Probe for Detection of Caspase Activities in Solutions. The distinct emission behavior of

dx.doi.org/10.1021/ja3064588 | J. Am. Chem. Soc. 2012, 134, 17972−17981

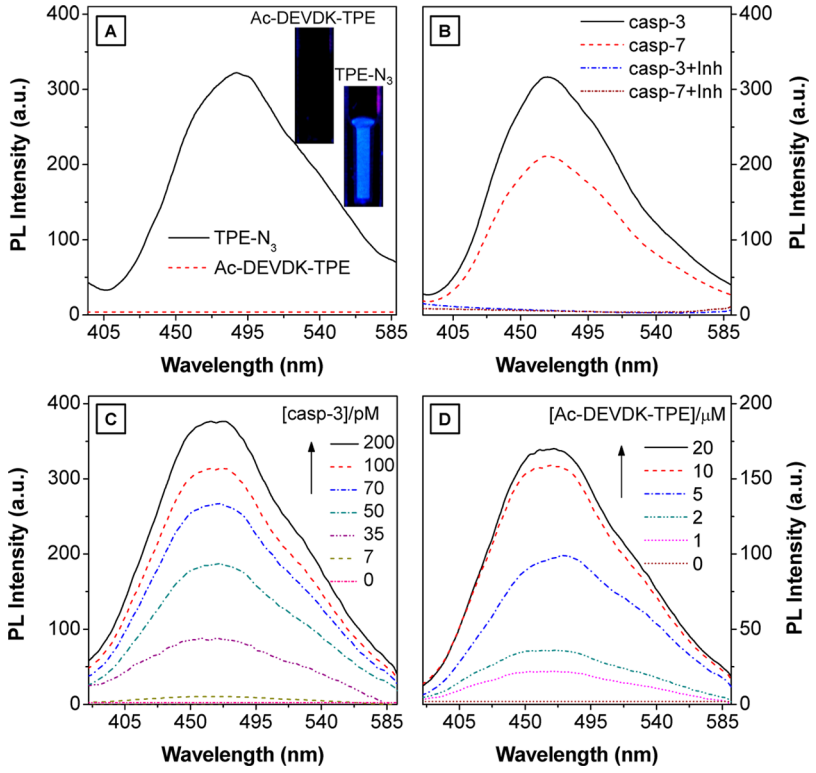

Figure 1. (A) Photoluminescence (PL) spectra of TPE-N_3 and Ac-DEVDK-TPE in DMSO/water (v/v = 1:199). Inset: photographs of TPE-N_3 and Ac-DEVDK-TPE in DMSO/water (v/v = 1:199) taken under illumination by an UV lamp. (B) PL spectra of Ac-DEVDK-TPE upon treatment with caspase-3 and -7 in the presence and absence of inhibitor 5-[(*S*)-(+)-2-(methoxymethyl)pyrrolidino]sulfonylisatin. (C) PL spectra of Ac-DEVDK-TPE in the presence of different amounts of caspase-3 (0, 7, 35, 50, 70, 100, and 200 pM). (D) PL spectra of different concentrations of Ac-DEVDK-TPE (0, 1, 2, 5, 10, and 20 μM) in the presence of caspase-3. The incubation time is 1 h. [TPE-N_3] = [Ac-DEVDK-TPE] = 10 μM; [caspase-3] = [caspase-7] = 100 pM; [inhibitor] = 10 μM; λ_{ex} = 312 nm.

Ac-DEVDK-TPE as compared to TPE itself prompted us to explore the potential of the probe for caspase activity study. We performed *in vitro* enzymatic assays with recombinant caspase-3/-7 first. Mixtures of Ac-DEVDK-TPE (10 μM) and caspases (100 pM) were prepared and incubated in piperazine-*N*,*N*′-bis(2-ethanesulfonic acid) (PIPES) buffer (50 mM PIPES, 100 mM NaCl, 1 mM ethylenediaminetetraacetic acid (EDTA), 0.1% w/v 3-[(3-cholamidopropyl)dimethylammonio] propanesulfonic, 25% w/v sucrose, pH = 7.2) at 37 °C. After 1 h incubation, the PL spectra were measured in the range from 360 to 620 nm. As shown in Figure 1B, strong fluorescence signals are recorded for the probe upon treatment with caspase-3/-7. However, most of the fluorescence is readily competed away by pretreatment of the probe with 5-[(*S*)-(+)-2-(methoxymethyl)pyrrolidino]sulfonylisatin, a highly specific inhibitor of caspase-3/-7,[35] indicating that specific cleavage of DEVD from Ac-DEVDK-TPE is inhibited. This is further confirmed by LC-MS as shown in Figure S11. After treatment with caspase-3, particles with an average diameter of 133 nm are formed along with the increase of solution fluorescence (Figure S12A).

To optimize the quantity of enzyme and probe used in the assays, different concentrations of caspase-3 ranging from 0 to 200 pM were incubated with Ac-DEVDK-TPE (10 μM) in PIPES buffer (pH = 7.2) for 1 h. Figure 1C shows the variation in the PL spectra of the assay. With the increasing concentrations of caspase-3, the PL intensities gradually increase due to the increased amount of TPE-K fluorogen (Φ = 0.07, Table S1) released, which emits strongly in aqueous solution. In comparison to the probe's intrinsic emission in the buffer solution, a 75-fold PL enhancement is observed when the probe is incubated with 200 pM caspase-3 for 1 h. Additionally, the PL intensities of the assay increase linearly with the increasing concentrations of caspase-3 (Figure S12B). Therefore, the hydrolysis kinetics of Ac-DEVDK-TPE catalyzed by caspase-3 can be easily studied on the basis of the PL intensity changes. Likewise, when recombinant caspase-3 (100 pM) is treated with different concentrations of Ac-DEVDK-TPE, a progressive fluorescence increase at 470 nm is also observed with increasing concentrations of Ac-DEVDK-TPE. As there is only slight fluorescence increase observed when the concentration of Ac-DEVDK-TPE is higher than 10 μM (Figure 1D), these data illustrate that 10 μM Ac-DEVDK-TPE is sufficient for digestion by 100 pM caspase-3. Therefore, 10 μM Ac-DEVDK-TPE and 100 pM caspase-3 were chosen as the optimal conditions for the following enzymatic experiments.

The enzyme kinetic studies were subsequently performed by incubating recombinant caspase-3/-7 with Ac-DEVDK-TPE in buffer at 37 °C, and the changes in fluorescence were monitored over time. As shown in Figure 2A, a significant increase in solution fluorescence over background is observed when caspase-3/-7 is used. In the absence of caspase-3/-7, no change in fluorescence is observed, confirming that Ac-DEVDK-TPE is specifically recognized and cleaved by caspase-3/-7. To further investigate the probe selectivity, Ac-DEVDK-TPE was treated with several proteins, such as caspase-3/-7, pepsin, bovine serum albumin (BSA), trypsin, and lysozyme, under identical conditions. As shown in Figure 2B, caspase-3/-7 display around 45- and 28-fold higher changes in $(I - I_0)/I_0$ than the other four proteins. This substantiates

dx.doi.org/10.1021/ja3064588 | *J. Am. Chem. Soc.* 2012, 134, 17972−17981

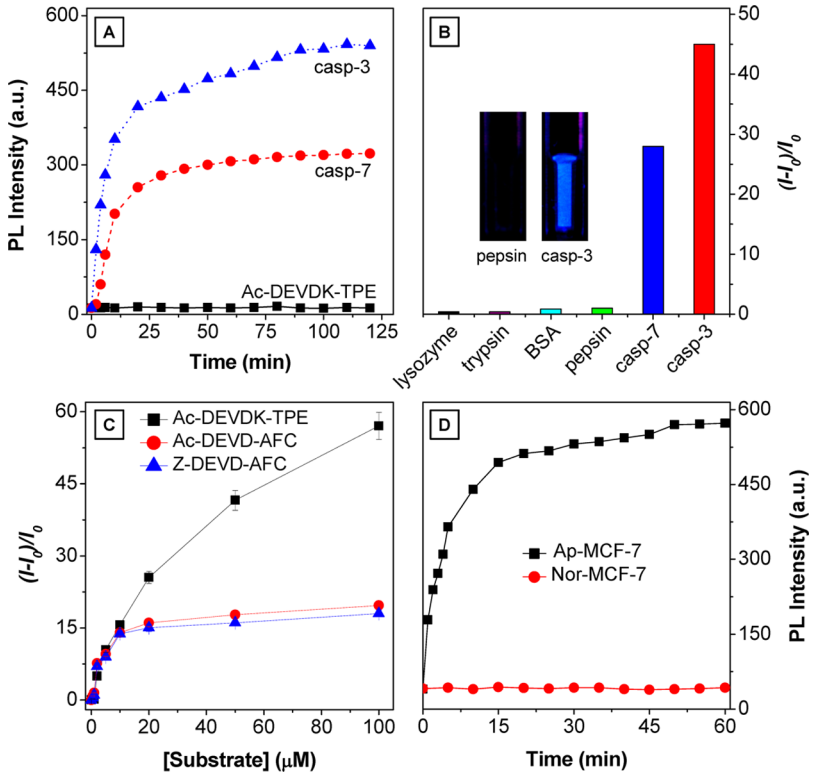

Figure 2. (A) Time-dependent PL spectra of Ac-DEVDK-TPE upon addition of caspase-3 and caspase-7 from 0 to 120 min. [caspase-3] = [caspase-7] = 100 pM. (B) Plot of $(I - I_0)/I_0$ versus different proteins, where I and I_0 are the PL intensities at protein concentrations of 100 and 0 pM, respectively. Inset: photographs of the corresponding solutions containing caspase-3 or pepsin taken under illumination by an UV lamp. The solutions containing other proteins (lysozyme, trypsin, and BSA) look the same as that of pepsin. (C) Plot of $(I - I_0)/I_0$ versus concentrations of Ac-DEVDK-TPE, Ac-DEVD-AFC, and Z-DEVD-AFC in PIPES buffer, where I and I_0 are the PL intensities of mixtures with or without substrates. (D) Time-dependent PL spectra of Ac-DEVDK-TPE in apoptotic MCF-7 cell lysate (Ap-MCF-7, black squares) and normal MCF-7 cell lysate (Nor-MCF-7, red circles). [Ac-DEVDK-TPE] = 10 μM; λ_{ex} = 312 nm.

that Ac-DEVDK-TPE is indeed a specific probe for caspase-3/-7.

Kinetic Analysis of Ac-DEVDK-TPE Cleavage. We next performed the kinetic analysis of Ac-DEVDK-TPE cleavage by caspase-3. Caspase-3 (100 pM) was incubated at 37 °C in 50 μL of PIPES buffer with increasing concentrations of Ac-DEVDK-TPE and two commercial coumarin-based caspase-3 substrates, Ac-DEVD-AFC and Z-DEVD-AFC (from 0 to 100 μM), in parallel. The fluorescence intensities at 470 or 500 nm were monitored over 60 min at 37 °C. Kinetic constants were computed by direct fitting of the data to the Michaelis–Menten equation, $V_0 = K_{cat}[E]_0[S]/K_m + [S]$, using a nonlinear regression via GraphPad Prism software.[36] The Michaelis constant K_m is a measure of the substrate's affinity to the enzyme; it is commonly used to evaluate the effect of modification on substrate. K_{cat}, the turnover number, is the maximum number of substrate molecules converted to product per enzyme molecule per second. The K_m and K_{cat} values of Ac-DEVDK-TPE against caspase-3 are 5.38 ± 0.03 μM and 17.1 ± 0.2 s^{-1}, respectively, which are apparently better than those of Ac-DEVD-AFC (K_m = 12.70 ± 0.02 μM and K_{cat} = 2.7 ± 0.1 s^{-1}) and Z-DEVD-AFC (K_m = 15.37 ± 0.01 μM and K_{cat} = 2.5 ± 0.3 s^{-1}) (Figure 2C; Figure S13 and Table S2). The higher binding affinity to caspase-3 and larger enzyme turnover number for Ac-DEVDK-TPE as compared to those for Ac-DEVD-AFC and Z-DEVD-AFC clearly indicate the great potentials of the developed probe for enzyme activity studies.

Owing to the essential roles caspase-3/-7 played in cellular apoptosis, we next assessed whether Ac-DEVDK-TPE could selectively monitor the caspase-3/-7 activity in complex cellular proteomes. Both normal and apoptotic MCF-7 cellular lysates were collected and directly treated with Ac-DEVDK-TPE, followed by fluorescence measurement in a time-dependent manner. No fluorescence increase is observed in the uninduced cellular lysates, while a typical saturation kinetic of enzymatic activity is observed for apoptotic lysates (Figure 2D). This is consistent with recombinant caspase-3/-7 shown in Figure 2A, which further demonstrates that the fluorescence is generated from catalytic cleavage of the substrate DEVD in Ac-DEVDK-TPE.

To explore the possibility of using Ac-DEVDK-TPE as a screening tool for caspase-3 inhibitors, we performed the competitive enzymatic assay with different amounts of 5-[(*S*)-(+)-2-(methoxymethyl)pyrrolidino]sulfonylisatin (Figure S14). Results show a dose-dependent decrease of fluorescence with a calculated IC_{50} value of 63.4 nM for the inhibitor, which is in good agreement with the literature value reported previously.[35] These results indicate that our probe has great capability for caspase inhibitor screening.

Imaging of Cell Apoptosis Using Ac-DEVDK-TPE. After investigating the response characteristics of Ac-DEVDK-TPE as a protease probe *in vitro*, we further explored the potential of the probe for live-cell imaging of caspase-3 activation. Cytotoxicity of Ac-DEVDK-TPE was first evaluated by the widely used MTT assay. As shown in Figure S15, after the

dx.doi.org/10.1021/ja3064588 | J. Am. Chem. Soc. 2012, 134, 17972–17981

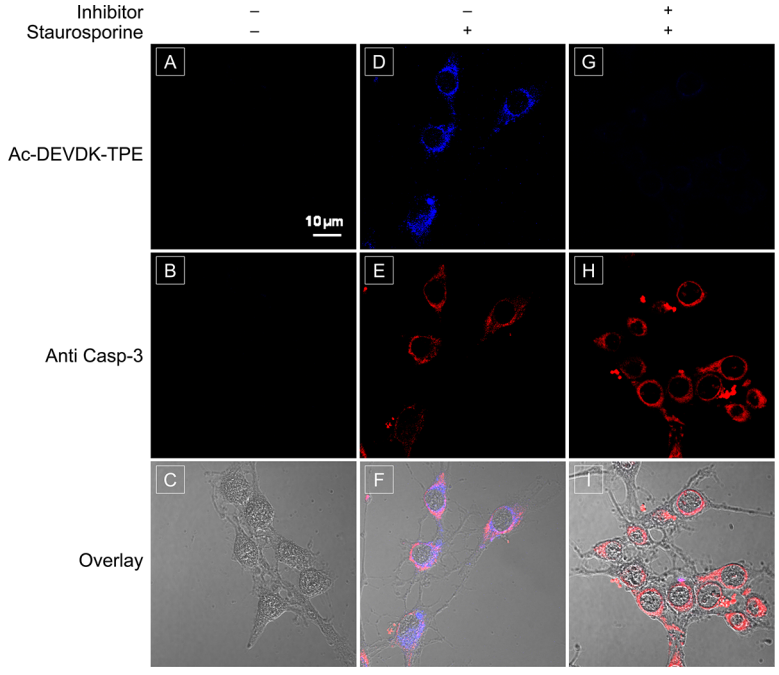

Figure 3. Fluorescence microscope images: (A–C) normal MCF-7 cells treated with Ac-DEVDK-TPE; (D–F) apoptotic MCF-7 cells treated with Ac-DEVDK-TPE (5 μM, 1% DMSO); (G–I) apoptotic MCF-7 cells treated with Ac-DEVDK-TPE (5 μM, 1% DMSO), inhibitor (10 μM), and caspase-3 antibody. Staurosporine (STS, 1 μM) was used to induce cell apoptosis. Blue, probe fluorescence; red, immunofluorescence signal generated from anti-caspase-3 primary antibody and a Texas Red-labeled secondary antibody. The images were acquired using a fluorescence microscope (Nikon) equipped with DAPI and Texas Red. All images share the same scale bar (10 μm).

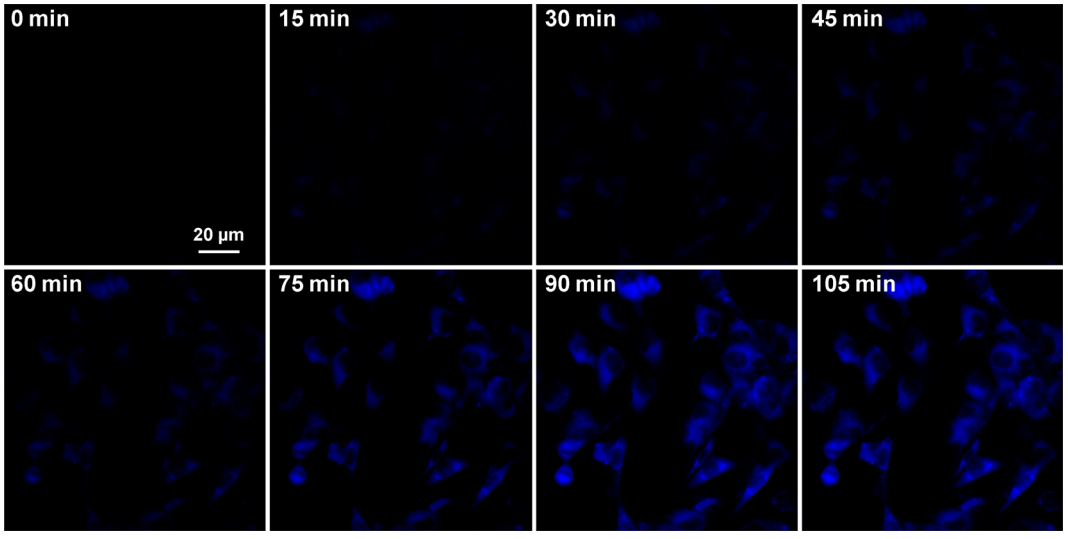

Figure 4. Real-time fluorescence images showing the cell apoptotic process of MCF-7 cells with Ac-DEVDK-TPE at room temperature. STS (1 μM) was used to induce cell apoptosis. The images were acquired using a fluorescence microscope (Nikon) equipped with a DAPI filter. All images have the same scale bar (20 μm). See the movie in the SI for the dynamic imaging process.

samples were incubated with 5, 10, or 25 μM Ac-DEVDK-TPE for 48 h, the cell viabilities are close to 100% under the testing conditions, indicative of low cytotoxicity of the probe. Fluorescence microscopy was used to image normal and apoptotic MCF-7 cells after treatment with Ac-DEVDK-TPE. MCF-7 cells were first incubated with Ac-DEVDK-TPE in DMEM for 2 h at 37 °C. The cells were subsequently treated with staurosporine (STS, 1 μM), a commonly used apoptosis inducer. After 1 h of incubation, Ac-DEVDK-TPE activation was determined by monitoring the fluorescence changes with fluorescence microscopy. As shown in Figures 3 and S16, normal, uninduced cells show an extremely low fluorescence signal, indicative of little or no caspase-3 activity (Figure 3A). In sharp contrast, strong fluorescence signals are collected from the cells treated with STS (Figure 3D). The signals are greatly reduced when STS-induced cells are pretreated with 5-[(*S*)-(+)-2-(methoxymethyl)pyrrolidino]sulfonylisatin, a commercial caspase-3/-7 inhibitor, before incubation with Ac-DEVDK-TPE (Figure 3G). Furthermore, excellent overlap is observed between the fluorescence images of the probe and immunofluorescence signals generated from anti-caspase-3 primary antibody and a Texas Red-labeled secondary antibody

dx.doi.org/10.1021/ja3064588 | *J. Am. Chem. Soc.* 2012, 134, 17972–17981

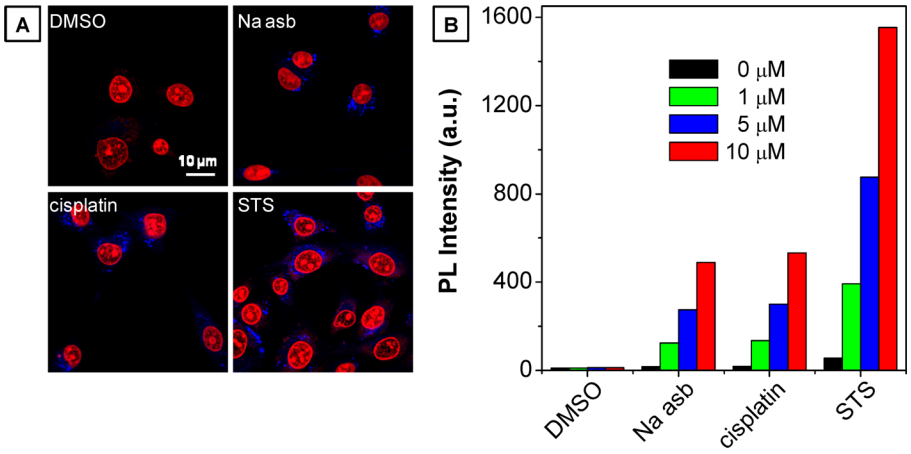

Figure 5. (A) Fluorescence microscope images of Ac-DEVDK-TPE-pre-incubated MCF-7 cells upon treatment with 1 μM each of DMSO, sodium ascorbate (Na asb), cisplatin, and staurosporine (STS). [Ac-DEVDK-TPE] = 5 μM. Nuclei were stained with propidium iodide (Invitrogen). The images were acquired using a fluorescence microscope (Nikon) equipped with DAPI and Texas Red filter. All images share the same scale bar (10 μm). (B) Photoluminescence (PL) intensities of Ac-DEVDK-TPE-pre-incubated MCF-7 cells upon treatment with different amounts of DMSO, Na asb, cisplatin, and STS. λ_{ex} = 312 nm; λ_{em} = 470 nm.

(Figure 3F). Additionally, apoptotic MCF-7 cells were treated with both Ac-DEVDK-TPE and commercial Annexin V-Alexa Fluor. As expected, Annexin V-Alexa Fluor is localized on the cell surface, but Ac-DEVDK-TPE shows strong fluorescence inside the cells (Figure S17). Collectively, these results provide direct evidence for intracellular delivery and caspase-specific activation of the imaging probe. Undoubtedly, Ac-DEVDK-TPE is a suitable probe for detection of caspase-3 activity and apoptosis imaging in live cells.

To explore whether our probe can be used for monitoring cell apoptosis, real-time imaging experiments were performed. Ac-DEVDK-TPE (5 μM) was first incubated with MCF-7 cells at 37 °C. After 2 h of incubation, the cells were treated with STS (1 μM) and monitored with fluorescence microscopy to obtain real-time fluorescence images. The dark background in each image shown in Figure 4 indicates that the probe is nonfluorescent in the cell culture media. As the incubation time elapses, the fluorescence intensity increases gradually with the cellular apoptotic progress, which reaches a maximum at 90 min. These results clearly demonstrate that Ac-DEVDK-TPE not only can be used for detection of caspase-3 activity but also has the potential for real-time monitoring of cell apoptosis.

***In Situ* Screening of Apoptosis-Inducing Agents.** The discovery of novel compounds that modulate apoptosis pathways could lead to the development of new anticancer agents. To assess the capability of our probe for *in situ* screening of compounds that can induce cell apoptosis, three known apoptosis inducers, sodium ascorbate,[37] cisplatin, and STS,[38] were used to treat MCF-7 cells. After the cells were incubated with Ac-DEVDK-TPE for 2 h, each compound (1 μM in DMSO) was added into the chamber for an additional 1.5 h incubation. The apoptosis-inducing capabilities of these agents were evaluated by monitoring the cell fluorescence increase with fluorescence microscopy. As shown in Figure 5A, a 35-fold fluorescence increase is observed for STS-treated cells compared to that for DMSO-treated cells, while only 11- and 12-fold increases are observed for sodium ascorbate- and cisplatin-treated cells, respectively. These results indicate that STS has a relatively high inducing efficacy for apoptosis, which is consistent with the literature report.[38] Therefore, our probe can potentially be used for screening apoptosis-inducing agents in living cells.

To further evaluate whether the probe can be used to quantify the efficacy of apoptosis-inducing agents, after incubation with Ac-DEVDK-TPE, MCF-7 cells were treated with different amounts of DMSO, sodium ascorbate, cisplatin, and STS for 2 h before the fluorescence measurement. As shown in Figure 5B, with increasing concentration of the compounds used, the cell fluorescence is progressively intensified. Among them, STS shows the best performance for apoptosis induction. Collectively, these results suggest that our probe can also be used for quantitative analysis of apoptosis-related drug efficacy in living cells.

■ CONCLUSIONS

In summary, a DEVD-conjugated AIE probe has been successfully developed in this work. Thanks to its novel AIE nature, the probe is nonfluorescent in aqueous buffers but becomes emissive when cleaved by caspase-3/-7. It enables light-up monitoring of caspase-3/-7 activities in solution and in cells with high signal-to-noise ratios, which shows superior performance over commercial coumarin-based fluorogenic probes. Additionally, our AIE probe strategy provides an efficient platform for real-time imaging of live cell apoptosis, which further allows *in situ* screening and quantification of apoptosis-inducing agents. In light of its simplicity, low cost, and high efficiency as a live cell apoptosis imaging probe, further tuning of the emission spectrum of AIE fluorogen to red and near-IR regions will facilitate the development of specific bioprobes for *in vivo* imaging of cell apoptosis and drug screening.

■ EXPERIMENTAL SECTION

General Information. BSA, lysozyme, pepsin, and trypsin were purchased from Sigma. Recombinant human caspase-3, caspase-7, and Ac-DEVD-AFC were purchased from R&D Systems. Z-DEVD-AFC and Annexin V-Alexa Fluor were purchased from Invitrogen. Inhibitor 5-[(*S*)-(+)-2-(methoxymethyl)pyrrolidino]sulfonylisatin was purchased from Calbiochem. Cleaved caspase-3 (Asp175) (5A1E) rabbit mAb (#9664) was purchased from Cell Signaling. Mouse anti-rabbit IgG-TR (sc-3917) was purchased from Santa Cruz. Fetal bovine serum (FBS) and trypsin-EDTA solution were purchased from Gibco (Lige

dx.doi.org/10.1021/ja3064588 | J. Am. Chem. Soc. 2012, 134, 17972−17981

Technologies, AG, Switzerland). STS was purchased from Biovision. Milli-Q water was supplied by a Milli-Q Plus System (Millipore Corp., USA). MCF-7 breast cancer cell line was provided by American Type Culture Collection. UV−vis absorption spectra were taken on a Milton Ray Spectronic 3000 array spectrophotometer. PL spectra were measured on a Perkin-Elmer LS 55 spectrofluorometer. All PL spectra were measured with an excitation wavelength of 312 nm. Average particle size and size distribution of TPE-N_3 and lysine-conjugated TPE (K-TPE) were determined by LLS with a particle size analyzer (90 Plus, Brookhaven Instruments Co., USA) at a fixed angle of 90° at room temperature. The cells were imaged by fluorescence microscopy (Nikon A1 confocal microscope).

Hexane and tetrahydrofuran were distilled from sodium benzophenone ketyl immediately prior to use. Dichloromethane (DCM) was distilled over calcium hydride. Diphenylmethane, *n*-butyllithium, 4-methylbenzophenone, *p*-toluenesulfonic acid, *N*-bromosuccinimide, benzoyl peroxide, copper(II) sulfate, sodium ascorbate, *N*,*N*-diisopropylethylamine (DIEA), DMSO, trifluoroacetic acid (TFA), triisopropylsilane (TIS), PIPES, EDTA, 3-[(3-cholamidopropyl)-dimethylammonio]propanesulfonic acid (CHAPS), hex-5-ynoic acid, and solvents were all purchased from Sigma-Aldrich and used as received without further purification. Rink-amide resin, *O*-benzotriazole-*N*,*N*,*N*′,*N*′-tetramethyluronium hexafluorophosphate (HBTU), *N*-hydroxybenzotriazole (HOBt), and Fmoc-protected amino acids were purchased from GL Biochem Ltd. ^{1}H and ^{13}C NMR spectra were measured on a Bruker ARX 400 NMR spectrometer. Chemical shifts were reported in parts per million (ppm) referenced with respect to residual solvent ($CDCl_3$ = 7.26 ppm, $(CD_3)_2SO$ = 2.50 ppm, or tetramethylsilane (TMS) $Si(CH_3)_4$ = 0 ppm). High-resolution mass spectra (HR-MS) were recorded on a Finnigan MAT TSQ 7000 mass spectrometer operating in MALDI-TOF mode. The HPLC profiles and ESI mass spectra were acquired using a Shimadzu IT-TOF. All HPLC experiments used 0.1% TFA/H_2O and 0.1% TFA/acetonitrile as eluents. The flow rate was 0.6 mL/min for analytical HPLC and 3 mL/min for preparative HPLC. Details of synthetic procedures and characterizations of compounds **1**, **2**, and **5** are reported in the Supporting Information. Characterizations of the key intermediates and Ac-DEVDK-TPE are reported below.

Synthesis of 1-((4-Azidomethyl)phenyl)-1,2,2-triphenylethene (3). In a 250 mL two-neck round-bottom flask, 1.70 g (4 mmol) of **2** and 0.39 g (6 mmol) of sodium azide were dissolved in DMSO under N_2. The mixture was stirred at room temperature overnight. A large amount (100 mL) of water was then added, and the solution was extracted three times with diethyl ether. The organic layers were combined, dried over magnesium sulfate, and concentrated. The crude product was purified by silica gel chromatography using hexane/chloroform (v/v = 3:1) as eluent to give **3** as a white solid (1.5 g, 97% yield). ^{1}H NMR ($CDCl_3$, 400 MHz), δ (TMS, ppm): 7.13−7.06 (m, 9H), 7.06−6.98 (m, 10H), 4.24 (s, 2H). ^{13}C NMR ($CDCl_3$, 100 MHz), δ (TMS, ppm): 143.27, 142.90, 142.83, 140.82, 139.62, 132.61, 131.22, 131.11, 130.67, 127.09, 127.04, 126.99, 126.02, 125.90, 53.91. HR-MS (MALDI-TOF): m/z 387.1342 [$(M)^+$, calcd 387.1735].

Synthesis, Purification, and Characterization of Ac-DEVDK-alkyne (Ac-DEVDK-A). Ac-DEVDK-A was synthesized using standard Fmoc strategy with rink amide resin as the solid support. Standard HOBt/HBTU/DIEA coupling method was used throughout the whole process.[18d] The resin (100 mg, loading ∼0.5 mmol/g) was swelled in HPLC-grade DMF for 1 h at room temperature. Subsequently, Fmoc group was deprotected in piperidine/DMF (v/v = 1/4) for 2 h at room temperature. Following piperidine removal, the resin was washed extensively with DMF and DCM and dried thoroughly under high vacuum. Next, alkyne-containing lysine **5** (Scheme S1) was dissolved in dry DMF (1.5 mL) together with HBTU (4 equiv), HOBt (4 equiv), and DIEA (8 equiv). The dry resin was then added, and the resulting mixture was shaken at room temperature. After overnight reaction, the resin was filtered and washed thoroughly with DMF (3×), DCM (3×), and DMF (3×) until the filtrate became colorless. After drying thoroughly under high vacuum, the resin was deprotected again with 20% piperidine in DMF for the next coupling cycle. The above cycle was repeated until the last amino acid has been coupled. Finally, the resin was capped with a solution of Ac_2O (10 equiv) and DIEA (20 equiv) in DCM (200 mL), and the mixture was allowed to react for 2 h at room temperature. After the whole coupling process, the resin was washed thoroughly with DMF and dried under high vacuum for 2 h at room temperature. The peptide was then cleaved in a mixture of 95% TFA, 2.5% TIS, and 2.5% H_2O for 4 h at room temperature. Following prolonged concentration *in vacuo* until >80% of cleavage cocktail was removed, cold ether (chilled to −20 °C) was added to the liquid residue to precipitate the peptide. The ether layer was then decanted, and the precipitates were dried thoroughly *in vacuo*. The resulting peptide was further purified by prep-HPLC and characterized by LC-MS (IT-TOF): m/z calcd 739.34, found 739.30. The HPLC condition is 20−100% B for 10 min, then 100% B for 2 min, 20% B for 5 min (solvent A = 100% H_2O with 0.1% TFA; solvent B = 100% CH_3CN with 0.1% TFA).

"Click" Synthesis of Probe Ac-DEVDK-TPE. Ac-DEVD-A (3.7 mg, 5 μmol) and TPE-N_3 (2.2 mg, 6 μmol) were dissolved in 50 μL of DMSO. A mixture of DMSO/H_2O solution (v/v = 1/1; 0.5 mL) was subsequently added, and the reaction was shaken for a few minutes to obtain a clear solution. The "click" reaction was initiated by sequential addition of catalytic amounts of sodium ascorbate (0.4 mg, 2.0 μmol) and $CuSO_4$ (1.6 mg, 1.0 μmol). The reaction was continued with shaking at room temperature for another 24 h. The final product was purified by prep-HPLC and further characterized by NMR and HRMS. ^{1}H NMR (400 MHz, DMSO-d_6), δ (TMS, ppm): 8.25 (d, J = 8.0 Hz, 1H), 8.17 (d, J = 8.0 Hz, 1H), 7.93 (d, J = 8.0 Hz, 1H), 7.81 (s, 1H), 7.73−7.67 (m, 3H), 7.12−6.95 (m, 21H), 5.42 (s, 2H), 4.55−4.50 (m, 2H), 4.29−4.24 (m, 1H), 4.12−4.04 (m, 2H), 2.98−2.94 (m, 2H), 2.74−2.70 (dd, J = 8.0 Hz, 1H), 2.65−2.60 (dd, J = 8.0 Hz, 1H), 2.57−2.42 (m, 5H, overlap with DMSO-d_6), 2.23−2.17 (m, 2H), 2.08 (t, J = 8.0 Hz, 2H), 1.93−1.89 (m, 2H), 1.82 (s, 3H), 1.77 (t, J = 8.0 Hz, 2H), 1.70−1.61 (m, 1H), 1.50−1.40 (m, 1H), 1.40−1.27 (m, 2H), 1.26−1.18 (m, 2H), 0.80 (m, 6H). ^{13}C NMR (100 MHz, DMSO-d_6), δ (TMS, ppm): 174.9, 174.3, 172.9, 172.6, 172.4, 171.9, 171.7, 171.6, 171.0, 170.4, 147.6, 143.9, 143.8, 141.8, 140.9, 135.1, 131.7, 131.4, 128.7, 128.1, 127.5, 127.4, 123.0, 58.4, 55.3, 53.1, 52.9, 50.4, 50.3, 39.3, 36.8, 36.5, 35.7, 32.3, 31.5, 30.9, 29.7, 27.9, 26.0, 25.5, 23.5, 23.3, 20.0, 18.8. HRMS (MALDI-TOF): m/z 1149.4998 ([M+Na]$^+$, calcd 1149.5124). HPLC conditions: 20−100% B for 10 min, then 100% B for 2 min, 20% B for 5 min (solvent A = 100% H_2O with 0.1% TFA; solvent B = 100% CH_3CN with 0.1% TFA).

General Procedure for Enzymatic Assay. DMSO stock solutions of Ac-DEVDK-TPE were diluted with caspase-3/-7 assay buffer (50 mM PIPES, 100 mM NaCl, 1 mM EDTA, 0.1% w/v CHAPS, 25% w/v sucrose, pH = 7.2) to make 10 μM working solutions. Next, 5 μL of the recombinant caspase-3/-7 (∼0.04 μg/μL stock solution in assay buffer) was added into the above working solution. The reaction mixture was incubated at room temperature for 60 min and then diluted to a total of 300 μL with deionized water for PL measurement. The solution was excited at 312 nm, and the emission was collected from 360 to 620 nm.

Cell Culture. MCF-7 cell lines were provided by American Type Culture Collection. MCF-7 breast cancer cells were cultured in DMEM (Invitrogen, Carlsbad, CA) containing 10% heat-inactivated FBS (Invitrogen), 100 U/mL penicillin, and 100 μg/mL streptomycin (Thermo Scientific) and maintained in a humidified incubator at 37 °C with 5% CO_2. Before experiment, the cells were precultured until confluence was reached.

Microscopy Imaging. MCF-7 cells were cultured in the chambers (LAB-TEK, Chambered Coverglass System) at 37 °C. After 80% confluence, the adherent cells were washed twice with 1× PBS buffer. The DEVDK-TPE solution (5 μM, 0.3 mL) was then added to the chamber. After incubation for 2 h at 37 °C, the cells were washed once with 1× PBS buffer and treated with 1 μM apoptosis inducers (STS, sodium ascorbate, and cisplatin) for 1 h. The cells were washed one time with 1× PBS buffer. For co-localization with Annexin V-Alexa Fluor, the cells were further incubated with a mixture of Annexin V-Alexa Fluor/FBS-free DMEM (v/v = 1:799) for 15 min at room

temperature and then washed once with 1× PBS buffer. The cells were then kept in fresh FBS-free DMEM for cell imaging. For co-localization with active caspase-3 antibody, the cells were first fixed for 15 min with 3.7% formaldehyde in 1× PBS at room temperature, washed twice with cold 1× PBS again, and permeabilized with 0.1% Triton X-100 in 1× PBS for 10 min. The cells were then blocked with 2% BSA in 1× PBS for 30 min and washed twice with 1× PBS. The cells were subsequently incubated with a mixture of anti-caspase-3 antibody/1× PBS (v/v = 1:99) for 1 h at room temperature, washed once with 1× PBS buffer, and then incubated with mouse anti-rabbit IgG-TR (0.8 μg mL^{-1}) in 1× PBS for 1 h, following by washing with 1× PBS again. The imaging was done with a fluorescence microscope (Nikon) equipped with DAPI, FITC, and Texas Red filters.

Real-Time Imaging of Cell Apoptosis. MCF-7 cells were cultured in the eight-well chambers (LAB-TEK, chambered coverglass system) at 37 °C. After 80% confluence, the adherent cells were washed twice with 1× PBS buffer. The DEVDK-TPE solution (5 μM, 0.3 mL) was then added to the chamber. After 2 h of incubation at 37 °C, the cells were washed twice with 1× PBS buffer, and STS (1 μM, 0.3 mL) was added to the chambers. The chambers were then placed on the microscope platform immediately, and the microscope was focused on a collection of cells. The fluorescence images at DAPI channel were acquired every 2 min.

Quantification of Cell Apoptosis by Fluorescence Microplate Reader. MCF-7 cells were seeded in 96-well plates (Costar, USA) at an intensity of 4×10^4 cells mL^{-1}. After 80% confluence, the medium was replaced by 10 μM Ac-DEVDK-TPE in FBS-free DMEM medium. After 2 h of incubation at 37 °C, the adherent cells were washed twice with 1× PBS buffer, and 100 μL aliquots of different concentrations of STS in DMEM were added into the wells. After an additional 2 h of incubation at 37 °C, the cells were washed once with 1× PBS buffer followed by fluorescence measurement using a T-CAN microplate reader. The excitation and emission wavelengths are 312 and 470 nm, respectively.

■ ASSOCIATED CONTENT

Ⓢ Supporting Information

Experimental procedures for intermediates; structural characterization data for TPE-N_3 and Ac-DEVDK-TPE; particle size distribution of TPE-N_3 and K-TPE; absorption spectra of TPE-N_3 and Ac-DEVDK-TPE; movie showing the dynamic process of cell apoptosis imaging. This material is available free of charge via the Internet at http://pubs.acs.org.

■ AUTHOR INFORMATION

Corresponding Author

cheliub@nus.edu.sg; tangbenz@ust.hk

Author Contributions

‡H.S. and R.T.K.K. contributed equally to this work.

Notes

The authors declare no competing financial interest.

■ ACKNOWLEDGMENTS

We thank the Singapore National Research Foundation (R-279-000-323-281), the Temasek Defense Systems Institute (R279-000-305-232/422/592), the Research Grants Council of Hong Kong (HKUST2/CRF/10and N_HKUST620/11), the Guangdong Innovative Research Team Program of China, and the Institute of Materials Research and Engineering of Singapore (IMRE/11-1C0213) for financial support.

■ REFERENCES

(1) Vaux, D. L.; Korsmeyer, S. J. *Cell* **1999**, *96*, 245−254.
(2) Grutter, M. *Curr. Opin. Struct. Biol.* **2000**, *10*, 649−655.
(3) Okada, H.; Mak, T. *Nat. Rev. Cancer.* **2004**, *4*, 592−603.
(4) Riedl, S. J.; Shi, Y. *Nat. Rev. Mol. Cell Biol.* **2004**, *5*, 897−907.
(5) Fischer, U.; Schulze-Osthoff, K. *Pharm. Rev.* **2005**, *57*, 187−215.
(6) (a) Shi, Y. *Nat. Struct. Biol.* **2001**, *8*, 394−401. (b) Niu, G.; Chen, X. *J. Nucl. Med.* **2010**, *51*, 1659−1662.
(7) Ran, S.; Thorpe, P. E. *Int. J. Radiat. Oncol. Biol. Phys.* **2002**, *54*, 1479−1484.
(8) Petrovsky, A.; Schellenberger, E.; Josephson, L.; Weissleder, R.; Bogdanov, A. J. *Cancer Res.* **2003**, *63*, 1936−1942.
(9) Schellenberger, E.; Bogdanov, A. J.; Hogemann, D.; Tait, J.; Weissleder, R.; Josephson, L. *Mol. Imaging.* **2002**, *1*, 102−107.
(10) Schellenberger, E.; Bogdanov, A. J.; Petrovsky, A.; Ntziachristos, V.; Weissleder, R.; Josephson, L. *Neoplasia* **2003**, *5*, 187−192.
(11) (a) Blankenberg, F. G.; Katsikis, P. D.; Tait, J. F.; Davis, R. E.; Naumovski, L.; Ohtsuki, K.; Kopiwoda, S.; Abrams, M. J.; Darkes, M.; Robbins, R. C.; Maecker, H. T.; Strauss, H. W. *Proc. Natl. Acad. Sci. U.S.A.* **1998**, *95*, 6349−6354. (b) Quinti, L.; Weissleder, R.; Tung, C. H. *Nano Lett.* **2006**, *6*, 488−490.
(12) Krysko, O.; de Ridder, L.; Cornelissen, M. *Apoptosis* **2004**, *9*, 495−500.
(13) Collins, R. J.; Harmon, B. V.; Gobe, G. C.; Kerr, J. F. R. *Int. J. Radiat. Biol.* **1992**, *61*, 451−453.
(14) Enright, H.; Hebbel, R. P.; Nath, K. A. *J. Lab. Clin. Med.* **1994**, *124*, 63−68.
(15) Thornberry, N.; Lazebnik, Y. *Science* **1998**, *281*, 1312−1316.
(16) Degterev, A.; Boyce, M.; Yuan, J. *Oncogene* **2003**, *22*, 8543−8567.
(17) Vaux, D. L.; Korsmeyer, S. J. *Cell* **1999**, *96*, 245−254.
(18) (a) Maxwell, D.; Chang, Q.; Zhang, X.; Barnett, E. M.; Piwnica-Worms, D. *Bioconjugate Chem.* **2009**, *20*, 702−709. (b) Dai, N.; Guo, J.; Teo, Y. N.; Kool, E. T. *Angew. Chem., Int. Ed.* **2011**, *50*, 5105−5109. (c) Huang, X. L.; Swierczewska, M.; Choi, K. Y.; Zhu, L.; Bhirde, A.; Park, J. W.; Kim, K.; Xie, J.; Niu, G.; Lee, K. C.; Lee, S.; Chen, X. Y. *Angew. Chem., Int. Ed.* **2012**, *51*, 1625−1630. (d) Hu, M.; Li, L.; Wu, H.; Su, Y.; Yang, P.-Y.; Uttamchandani, M.; Xu, Q. H.; Yao, S. Q. *J. Am. Chem. Soc.* **2011**, *133*, 12009−12020.
(19) (a) Bardet, P. L.; Kolahgar, G.; Mynett, A.; Miguel-Aliaga, I.; Briscoe, J.; Meier, P.; Vincent, J. P. *Proc. Natl. Acad. Sci. U.S.A.* **2008**, *105*, 13901−13905. (b) Kanno, A.; Yamanaka, Y.; Hirano, H.; Umezawa, Y.; Ozawa, T. *Angew. Chem., Int. Ed.* **2007**, *46*, 7595−7599. (c) Laxman, B.; Hall, D. E.; Bhojani, M. S.; Hamstra, D. A.; Chenevert, T. L.; Ross, B. D.; Rehemtulla, A. *Proc. Natl. Acad. Sci. U.S.A.* **2002**, *99*, 16551−16555.
(20) Diamond, S. L. *Curr. Opin. Chem. Biol.* **2007**, *11*, 46−51.
(21) (a) Lee, S.; Choi, K. Y.; Chung, H.; Ryu, J. H.; Lee, A.; Koo, H.; Youn, I. C.; Park, J. H.; Kim, I. S.; Kim, S. Y.; Chen, X.; Jeong, S. Y.; Kwon, I. C.; Kim, K.; Choi, K. *Bioconjugate Chem.* **2011**, *22*, 125−131. (b) Barnett, E. M.; Zhang, X.; Maxwell, D.; Chang, Q.; Piwnica-Worms, D. *Proc. Natl. Acad. Sci. U.S.A.* **2009**, *106*, 9391−9396. (c) Sun, I. C.; Lee, S.; Koo, H.; Kwon, I. C.; Choi, K.; Ahn, C. H.; Kim, K. *Bioconjugate Chem.* **2010**, *21*, 1939−1942. (d) Kim, K.; Lee, M.; Park, H.; Kim, J. H.; Kim, S.; Chung, H.; Choi, K.; Kim, I. S.; Seong, B. L.; Kwon, I. C. *J. Am. Chem. Soc.* **2006**, *128*, 3490−3491. (e) Bullok, K.; Piwnica-Worms, D. *J. Med. Chem.* **2005**, *48*, 5404−5407.
(22) (a) Lin, S. Y.; Chen, N. T.; Sun, S. P.; Chang, J. C.; Wang, Y. C.; Yang, C. S.; Lo, L. W. *J. Am. Chem. Soc.* **2010**, *132*, 8309−8315. (b) Boeneman, K.; Mei, B. C.; Dennis, A. M.; Bao, G.; Deschamps, J. R.; Mattoussi, H.; Medintz., I. L. *J. Am. Chem. Soc.* **2009**, *131*, 3828−3829.
(23) Lovell, J. F.; Chan, M. W.; Qi, Q. C.; Chen, J.; Zheng., G. *J. Am. Chem. Soc.* **2011**, *133*, 18580−18582.
(24) Luo, J.; Xie, Z.; Lam, J. W. Y.; Cheng, L.; Chen, H.; Qiu, C.; Kwok, H. S.; Zhan, X.; Liu, Y.; Zhu, D.; Tang, B. Z. *Chem. Commun.* **2001**, 1740−1741.
(25) (a) Hong, Y. N.; Lam, J. W. Y.; Tang, B. Z. *Chem. Commun.* **2009**, 4332−4353. (b) Wang, M.; Zhang, G.; Zhang, D. Q.; Zhu, D. B.; Tang, B. Z. *J. Mater. Chem.* **2010**, *20*, 1858−1867. (c) Hong, Y.; Lam, J. W. Y.; Tang, B. Z. *Chem. Soc. Rev.* **2011**, *40*, 5361−5388. (d) Tong, H.; Hong, Y. N.; Dong, Y. Q.; Ha1ussler, M.; Li, Z.; Lam, J. W. Y.; Dong, Y. P.; Sung, H. H.-Y.; Williams, I. D.; Tang, B. Z. *J. Phys. Chem. B* **2007**, *111*, 11817−11823.

(26) (a) Chen, J. W.; Law, C. C. W.; Lam, J. W. Y.; Dong, Y. P.; Lo, S. M. F.; Williams, I. D.; Zhu, D. B.; Tang, B. Z. *Chem. Mater.* **2003**, *15*, 1535−1546. (b) Li, Z.; Dong, Y.; Mi, B.; Tang, Y.; Haussler, M.; Tong, H.; Dong, Y.; Lam, J. W. Y.; Ren, Y.; Sung, H. H. Y.; Wong, K. S.; Gao, P.; Williams, I. D.; Kwok, H. S.; Tang, B. Z. *J. Phys. Chem. B* **2005**, *109*, 10061−10066. (c) Zhao, Z.; Wang, Z.; Lu, P.; Chan, C. Y. K.; Liu, D.; Lam, J. W. Y.; Sung, H. Y.; Williams, I. D.; Ma, Y.; Tang, B. Z. *Angew. Chem., Int. Ed.* **2009**, *48*, 7608−7611.

(27) (a) Liu, Y.; Tang, Y.; Barashkov, N. N.; Irgibaeva, I. S.; Lam, J. W. Y.; Hu, R.; Birimzhanova, D.; Yu, Y.; Tang, B. Z. *J. Am. Chem. Soc.* **2010**, *132*, 13951−13953. (b) Wang, M.; Zhang, D. Q.; Zhang, G. X.; Zhu, D. B. *Chem. Commun.* **2008**, 4469−4471. (c) Liu, Y.; Deng, C. M.; Tang, L.; Qin, A. J.; Hu, R. R.; Sun, J. Z.; Tang, B. Z. *J. Am. Chem. Soc.* **2011**, *133*, 660−663. (d) Hong, Y.; Meng, L. M.; Chen, S. J.; Leung, C. W. T.; Da, L.-T.; Faisal, M.; Silva, D.-A.; Liu, J. Z.; Lam, J. W. Y.; Huang, X. H.; Tang, B. Z. *J. Am. Chem. Soc.* **2012**, *134*, 1680−1689. (e) Shi, H.; Liu, J. Z.; Geng, J. L.; Tang, B. Z.; Liu, B. *J. Am. Chem. Soc.* **2012**, *134*, 9569−9572.

(28) Hatano, K.; Saeki, H.; Yokota, H.; Aizawa, H.; Koyama, T.; Matsuoka, K.; Terunuma, D. *Tetrahedron Lett.* **2009**, *50*, 5816−5819.

(29) (a) Qin, W.; Ding, D.; Liu, J. Z.; Wang, Z. Y.; Hu, Y.; Liu, B.; Tang, B. Z. *Adv. Funct. Mater.* **2012**, *22*, 771−779. (b) Yu, Y.; Feng, C.; Hong, Y. N.; Liu, J. Z.; Chen, S. J.; Ng, K. M.; Luo, K. Q.; Tang, B. Z. *Adv. Mater.* **2011**, *23*, 3298−3302. (c) Zhao, Q. L.; Li, K.; Chen, S. J.; Qin, A. J.; Ding, D.; Zhang, S.; Liu, Y.; Liu, B.; Sun, J. Z.; Tang, B. Z. *J. Mater. Chem.* **2012**, *22*, 15128−15135. (d) Geng, J. L.; Li, K.; Ding, D.; Zhang, X. H.; Qin, W.; Liu, J. Z.; Tang, B. Z.; Liu, B. *Small* **2012**, DOI: 10.1002/smll.201200814.

(30) (a) Zhao, Z.; Chen, S.; Lam, J. W. Y.; Lu, P.; Wang, Z.; Hu, B.; Chen, X.; Lu, P.; Kwok, H. S.; Ma, Y.; Tang, B. Z. *J. Mater. Chem.* **2011**, *21*, 10949−10956. (b) Liu, Y.; Chen, S.; Lam, J. W. Y.; Lu, P.; Kwok, R. T. K.; Mahtab, F.; Kwok, H. S.; Tang, B. Z. *Chem. Mater.* **2011**, *23*, 2536−2544.

(31) Xu, J. P.; Fang, Y.; Song, Z. G.; Mei, J.; Jia, L.; Qin, A. J.; Sun, J. Z.; Ji, J.; Tang, B. Z. *Analyst* **2011**, *136*, 2315−2321.

(32) Wang, M.; Gu, X. G.; Zhang, G. X.; Zhang, D. Q.; Zhu, D. B. *Anal. Chem.* **2009**, *81*, 4444−4449.

(33) Zhao, M. C.; Wang, M.; Liu, H. J.; Liu, D. S.; Zhang, G. X.; Zhang, D. Q.; Zhu, D. B. *Langmuir* **2009**, *25*, 676−678.

(34) Peng, L. H.; Zhang, G. X.; Zhang, D. Q.; Xiang, J. F.; Zhao, R.; Wang, Y. L.; Zhu, D. B. *Org. Lett.* **2009**, *11*, 4014−4017.

(35) Lee, D.; Long, S. A.; Adams, J. L.; Chan, G.; Vaidya, K. S.; Francis, T. A.; Kikly, K; Winkler, J. D.; Sung, C.-M.; Debouck, C.; Richardson, S.; Levy, M. A.; DeWolf, W. E.; Keller, P. M.; Tomaszek, T.; Head, M. S.; Ryan, M. D.; Haltiwanger, R. C.; Liang, P.-H.; Janson, C. A.; McDevitt, P. J.; Johanson, K.; Concha, N. O.; Chan, W.; Abdel-Meguid, S. S.; Badger, A. M.; Lark, M. W.; Nadeau, D. P.; Suva, L. J.; Gowen, M.; Nuttallk, M. E. *J. Biol. Chem.* **2000**, *275*, 16007−16014.

(36) Lehninger, A. L.; Nelson, D. L.; Cox, M. M. *Lehninger Principles of Biochemistry*; W. H. Freeman: New York, 2005; ISBN 978-0-7167-4339-2.

(37) Kang, J. S.; Cho, D.; Kim, Y. I.; Hahm, E.; Kim, Y. S.; Jin, S. N.; Kim, H. N.; Kim, D.; Hur, D.; Par, H.; Wang, Y. I.; Lee, W. J. *J. Cell. Physiol.* **2005**, *204*, 192−197.

(38) Herrmann, R.; Fayad, W.; Schwarz, S.; Berndtsson, M.; Linder, S. *J. Biomol. Screen.* **2008**, *13*, 1−8.